



HAL
open science

The Influence of the Magnetic Tip on Heterodimers in ESR-STM

Xue Zhang, Jose Reina-Gálvez, Christoph Wolf, Yu Wang, Hervé Aubin,
Andreas J Heinrich, Taeyoung Choi

► **To cite this version:**

Xue Zhang, Jose Reina-Gálvez, Christoph Wolf, Yu Wang, Hervé Aubin, et al.. The Influence of the Magnetic Tip on Heterodimers in ESR-STM. ACS Nano, 2023, 17 (17), pp.16935 - 16942. 10.1021/acsnano.3c04024 . hal-04281456

HAL Id: hal-04281456

<https://hal.science/hal-04281456>

Submitted on 14 Nov 2023

HAL is a multi-disciplinary open access archive for the deposit and dissemination of scientific research documents, whether they are published or not. The documents may come from teaching and research institutions in France or abroad, or from public or private research centers.

L'archive ouverte pluridisciplinaire **HAL**, est destinée au dépôt et à la diffusion de documents scientifiques de niveau recherche, publiés ou non, émanant des établissements d'enseignement et de recherche français ou étrangers, des laboratoires publics ou privés.

1 The Influence of the Magnetic Tip on Hetero-dimers
2 in ESR-STM

3 *Xue Zhang,^{1,2,3} Jose Reina-Gálvez,^{1,2} Christoph Wolf,^{1,2} Yu Wang,^{1,2} Hervé Aubin,⁴ Andreas J.*
4 *Heinrich,^{1,5,*} and Taeyoung Choi^{5,*}*

5 1 Center for Quantum Nanoscience, Institute for Basic Science (IBS), Seoul 03760, Republic of
6 Korea

7 2 Ewha Womans University, Seoul 03760, Republic of Korea

8 3 Spin-X Institute, School of Microelectronics, South China University of Technology,
9 Guangzhou 511442, China

10 4 Universités Paris-Saclay, CNRS, Centre de Nanosciences et de Nanotechnologies, 91120,
11 Palaiseau, France

12 5 Department of Physics, Ewha Womans University, Seoul 03760, Republic of Korea

13 KEYWORDS

14 exchange coupling, magnetic tip, hetero-dimers, electron spin resonance, scanning tunneling
15 microscopy

16

1 ABSTRACT

2 Investigating the quantum properties of individual spins adsorbed on surfaces by electron spin
3 resonance combined with scanning tunneling microscopy (ESR-STM) has shown great potential
4 for the development of quantum information technology at the atomic scale. A magnetic tip
5 exhibiting high spin-polarization is critical for performing an ESR-STM experiment. While the
6 tip has been conventionally treated as providing a static magnetic field in ESR-STM, it was
7 found that the tip can exhibit bi-stability, influencing ESR spectra. Ideally, the ESR splitting
8 caused by magnetic interaction between two spins on a surface should be independent of the tip.
9 However, we found that the measured ESR splitting of a metal atom-molecule hetero-dimer can
10 be tip-dependent. Detailed theoretical analysis reveals that this tip-dependent ESR splitting is
11 caused by a different interaction energy between the tip and each spin of the hetero-dimer. Our
12 work provides a comprehensive reference for characterizing tip features in ESR-STM
13 experiments and highlights the importance of employing a proper physical model when
14 describing the ESR tip, in particular, for hetero-spin systems.

15 INTRODUCTION

16 Utilizing individual spins as fundamental storage and computation units is of intense interests
17 in the era of quantum information science. Well-known approaches, such as optical manipulation
18 of nitrogen-vacancy defects in diamond^{1,2} and trapped ions^{3,4}, magnetic control over quantum
19 dots in semi- and superconducting circuits^{5,6}, and electrical control over single-molecule-magnet
20 in break junctions^{7,8}, have been extensively explored to develop innovative quantum information
21 technology. Recently, single spins adsorbed on surfaces have been employed for quantum-
22 coherent control using STM combined with electron spin resonance (ESR-STM)⁹⁻¹⁷, which

1 provides the unique opportunity to position individual spins and build nanostructures with
2 atomic-scale precision.

3 In an ESR-STM setup, an ac voltage at microwave frequency is applied to the tunneling
4 junction to drive the spin in resonance between its ground and excited states. So far, ESR-STM
5 has been employed to investigate various magnetic phenomena such as spin-spin interactions^{18,19},
6 hyperfine structures^{20,21} and coherent quantum control^{10,14}. In addition to the microwave, another
7 critical element for performing ESR-STM measurements is the magnetic tip, which is used to
8 read out the spin signal and drive the resonance.²² The tip is required to exhibit sufficient spin-
9 polarization to identify the spin-polarized tunneling current of different spin states via the
10 tunneling magneto-resistance effect.^{23,24} One of the methods to create an ESR-active tip in-situ is
11 to transfer a few magnetic atoms such as iron (Fe) onto the apex of a non-magnetic metallic tip
12 using atom manipulation in an external magnetic field. The Fe clusters can be magnetized and
13 ideally behave like a static magnet, as illustrated by previous studies²⁵⁻²⁷, where the tip is
14 considered as an additional source of an external magnetic field. Although characterizing the
15 detailed tip structure is highly challenging, it is of vital importance to understand the impact of
16 the magnetic characteristics of the tip on ESR spectra. In this work, we provide a detailed
17 analysis of magnetic stability and orientation of different ESR tips by comparing two spin-1/2
18 systems, iron-phthalocyanine (FePc) molecule and hydrogenated titanium atom (simply referred
19 as Ti in the following texts) adsorbed on an insulating surface. In addition, we found the
20 magnetic interaction between tip and each spin in a FePc-Ti hetero-dimer can be significantly
21 different depending on tip characteristics, resulting in a pronounced tip-dependent ESR splitting
22 in such hetero-dimers. Our work highlights that understanding the behavior of the magnetic tip is
23 critical for the reliable analysis of ESR spectra when using the ESR-STM technique.

1 RESULTS AND DISCUSSION

2 Thin MgO film with double layer thickness was prepared atop clean Ag(100). FePc molecules,
3 Ti and iron (Fe) atoms were sublimated onto MgO with a low coverage, as shown in Figure 1a.
4 Ti atoms exclusively adsorb on the bridge sites (between two oxygen atoms) and are marked as
5 Ti. To perform an ESR measurement, an oscillating radio-frequency electric voltage (V_{rf}) is
6 added to the dc voltage (V_{dc}). A typical ESR set-up is depicted in Figure 1b.^{9,23} After transferring
7 3~5 Fe atoms from the surface to the apex of the Pt/Ir tip, the tip becomes magnetic and ESR-
8 active and thus can detect the ESR signal via spin-polarized tunneling.^{23,24}

9 In most cases, the time-averaged effective spin of the magnetic cluster on the tip $\langle \mathbf{S}_{\text{tip}} \rangle$ has
10 been shown to behave Ising-like (*e.g.* having two distinct states “up” and “down”),²⁴⁻²⁷ and its
11 exchange interaction with the underneath spin can be approximated as an effective magnetic
12 field $\mathbf{B}_{\text{tip}} = J_{\text{tip}} \langle \mathbf{S}_{\text{tip}} \rangle / g\mu_B$.^{22,27} This implies that the interaction between the magnetic tip and
13 the surface spin can be expressed as effective magnetic field \mathbf{B}_{tip} .^{22,26,27} The sum of \mathbf{B}_{tip} and the
14 applied external magnetic field, \mathbf{B}_{ex} , determines the Zeeman energy of the surface spin. \mathbf{B}_{ex} is
15 applied in the out-of-plane direction z throughout our experiment and is much larger than \mathbf{B}_{tip} .
16 Therefore, we consider only the out-of-plane components of all magnetic variables ($\mathbf{B}_{\text{tip}} = \mathbf{B}_z$).

17 To demonstrate the role of a well-prepared magnetic tip in ESR-STM, we first performed ESR
18 measurements on individual FePc and Ti spins.^{13,25,28} For a spin-1/2 system, the resonance
19 frequency f_0 is related to the external magnetic field \mathbf{B}_{ex} through the relation:

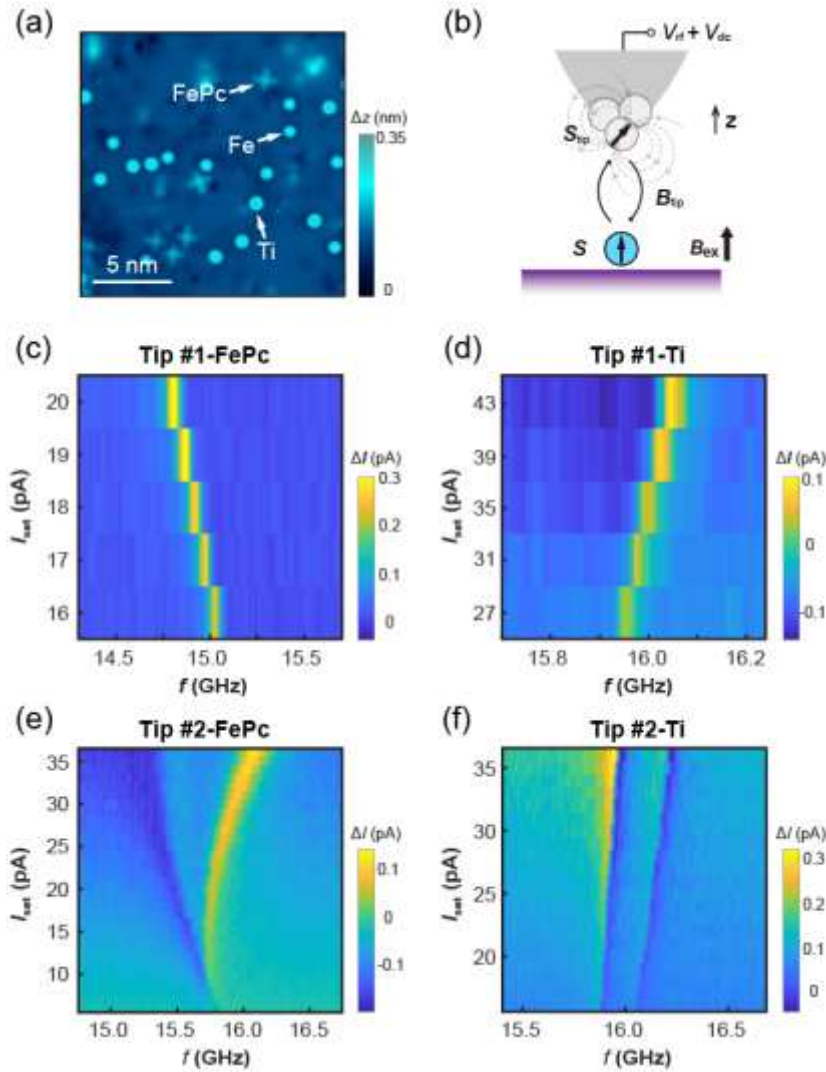
$$20 \quad hf_0 = 2\mu(\mathbf{B}_{\text{tip}} + \mathbf{B}_{\text{ex}}) \quad (1)$$

21 where h is Planck’s constant and μ is the magnetic moment of the spin. According to previous
22 ESR-STM studies,^{25,28,29} f_0 shifts linearly with the tunneling current (I_{set}) as well as \mathbf{B}_{tip} . This
23 implies that the magnetic interaction between the tip and the surface spins is dominantly

1 exchange-coupled since both \mathbf{B}_{tip} and the current exponentially depend on the tip height.
2 Therefore, we usually observe a linear shift of f_0 with tunneling current as shown in Figure 1c
3 and (d). Depending on the relative sign of \mathbf{B}_{tip} with respect to the \mathbf{B}_{ex} , f_0 can shift to lower or
4 higher frequencies for the tip being antiferromagnetically (AFM) or ferromagnetically (FM)
5 coupled to \mathbf{B}_{ex} , which allows to label them as AFM tip or FM tip, respectively. Notably, for the
6 same tip, the sign of \mathbf{B}_{tip} can sometimes depend on the measured type of surface spin. For
7 instance, tip#1 exhibits AFM type behavior on FePc (Figure 1c) but FM feature on Ti (Figure
8 1d). This observation already strongly suggests that treating the tip as a static magnet is an over
9 simplification and not suitable when the interaction with the surface spin can induce a change of
10 the relative orientation of the tip state. This interaction strength will be very sensitive to the
11 distance between the tip and the surface spin. Here, we found that the tip height on FePc and Ti
12 differ by ~ 0.17 nm, which may cause a change in the magnetic states of the tip due to proximity
13 of the surface spin.³⁰ We emphasize that there were neither changes in STM topographic images
14 nor in ESR spectra during the experiment, indicating that the magnetic microstructure of the tip
15 was unchanged.

16 In addition, about 30% of ESR tips can generate two peaks in the ESR spectrum although we
17 measure well-isolated individual spin-1/2s, as shown in Figure 1e and f. In contrast to tip#1, we
18 found that tip#2 displays two peaks for both FePc and Ti. We attribute this to the magnetic
19 bistability of the tip, which has been reported previously.^{27,31} In the case of the bistable tip, we
20 usually observe two peaks of an individual spin that shift as a function of the tip field (Figure 1e,
21 f and Figure S2). This can be well understood to occur under two conditions: First, the tip flips
22 the sign of its magnetic state (pointing to opposite direction) or changes its magnitude (whilst
23 maintaining the general direction). Second, the sign-change or magnitude-change event occurs at

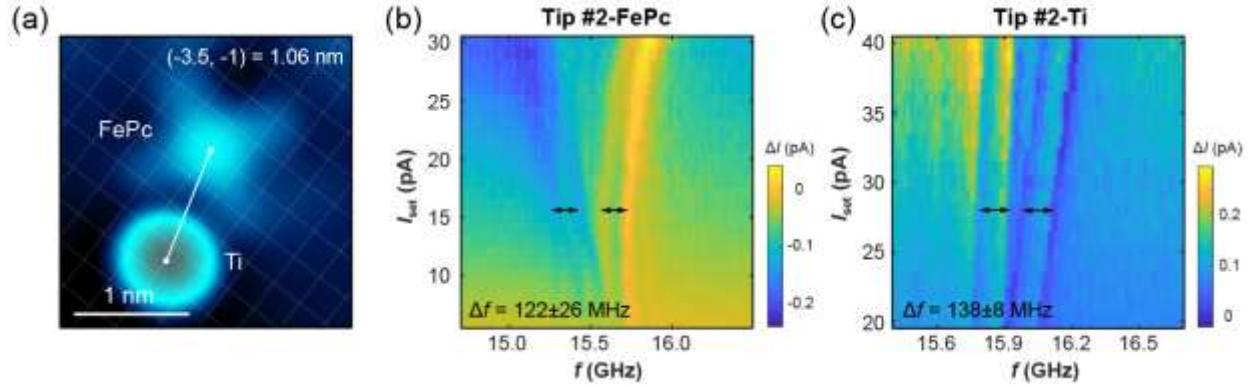
1 a time scale slower than the relaxation time of the tip state (\sim tens of nanoseconds) and faster than
 2 the ESR frequency sweep time (seconds), respectively.^{27,31} We note that the resonance shift of
 3 FePc measured by tip#2 deviates from a linear relationship with the current. This may be caused
 4 by a non-negligible magnetic dipolar interaction between the tip and FePc.



5
 6 **Figure 1. ESR measurements of individual FePc and Ti spins using different tips.** (a) STM
 7 image showing co-deposited FePc molecules (cross-like shape), Ti (bigger spot) and Fe (smaller
 8 spot) atoms on 2 ML MgO atop Ag(100) substrate. STM conditions: $V_{dc} = 200$ mV, $I_{set} = 10$ pA.
 9 (b) Schematic of ESR-STM junction consisting of a metallic tip decorated by several Fe atoms, a

1 molecular/atomic spin under the tip and the substrate below. The total magnetic field acting on
2 the surface spin consists of an effective tip field (B_{tip}) and the external field (B_{ex}). The
3 superposed rf and dc voltage (V_{rf} and V_{dc}) is applied to the tip while the sample is grounded. (c,
4 d) and (e, f) display the current dependence of ESR spectra plotted in color-scale of an individual
5 FePc spin and a Ti spin measured with tip#1 and tip#2, respectively. The tip is positioned above
6 the center of FePc and Ti for all ESR measurements. ESR conditions: $B_{\text{ex}} =$ (c, d) 560 mT, (e, f)
7 570 mT; $V_{\text{dc}} = 100$ mV; $V_{\text{rf}} =$ (c) 20 mV, (d, e) 30 mV, (f) 40 mV.

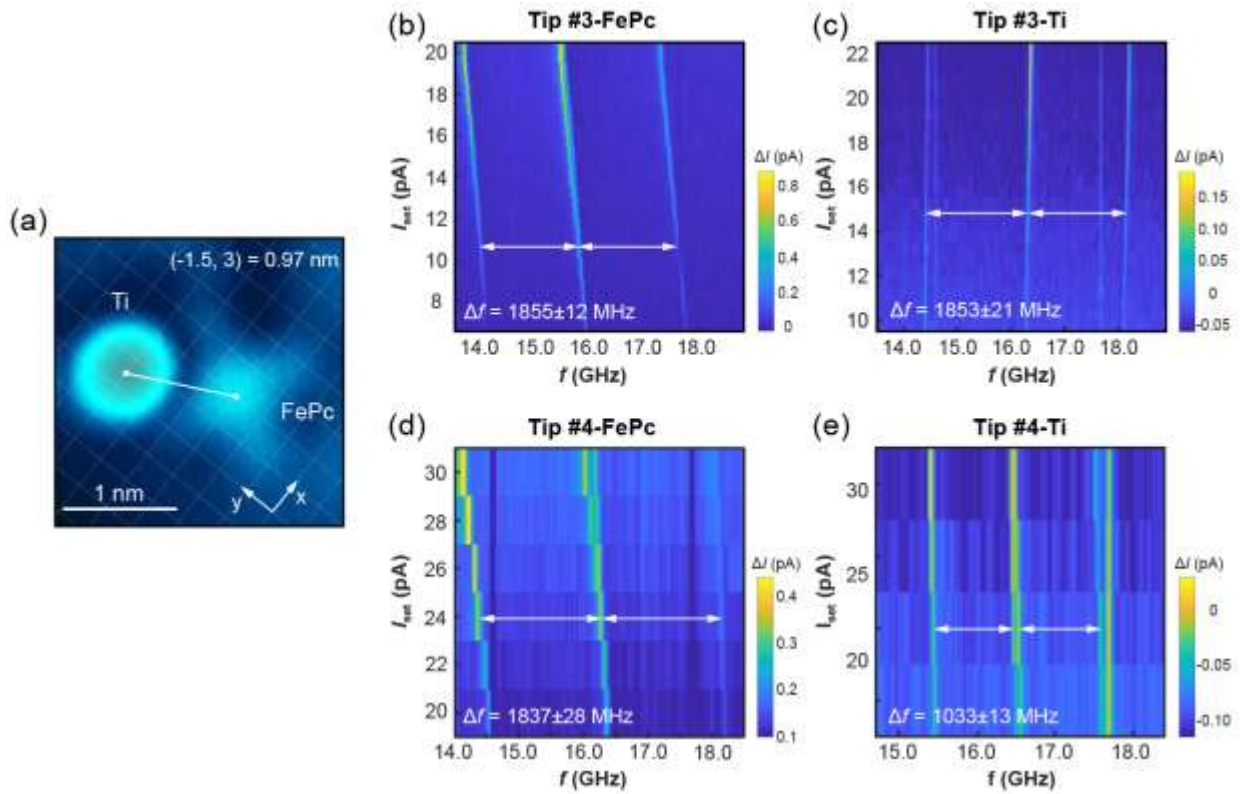
8 The bistable tip doubles the number of ESR peaks, which can be understood easily for
9 individual surface spins. However, the complex tip effects in multi-spin systems become non-
10 trivial. Already in two coupled spins of $S = 1/2$ (the spin states of each spin are denoted as $|0\rangle$
11 and $|1\rangle$), measured on a FePc-Ti pair in our experiment, the ESR spectrum displays four ESR
12 peaks (Figure 2), which might be assigned to the transitions between single-triplet states.
13 However, careful investigation of the spectra on individual spins (Figure S2) and spin pairs
14 (Figure S3-4) under various tip conditions revealed that the four ESR peaks simply arise from
15 the doubling of spin transitions ($|00\rangle \rightarrow |10\rangle \otimes |\uparrow\rangle$, $|00\rangle \rightarrow |10\rangle \otimes |\downarrow\rangle$ and equally for $|01\rangle \rightarrow$
16 $|11\rangle$), which flip Zeeman states of the two surface spins under two different tip states (we denote
17 the two tip states as $|\uparrow\rangle$ and $|\downarrow\rangle$). We note that the careful analysis on the tip enables us to
18 determine whether a particular ESR-active tip couples antiferromagnetically or ferromagnetically
19 to the surface spins, or is bistable by monitoring the direction of ESR peak shifting with tip
20 height as well as by monitoring the number of ESR peaks.



1
 2 **Figure 2. Doubling of ESR peaks of a FePc-Ti dimer measured with a bistable tip.** (a) STM
 3 image of a (3.5, 1) FePc-Ti dimer. Scanning conditions: $V_{dc} = 150$ mV, $I_{set} = 20$ pA. (b, c)
 4 Current dependence of ESR spectra measured on the dimer shown in (a) with the bistable tip#2
 5 on FePc and TiB, respectively. ESR conditions: $B_{ex} = 570$ mT; $V_{dc} = 100$ mV; $V_{rf} =$ (b) 30 mV,
 6 (c) 40 mV.

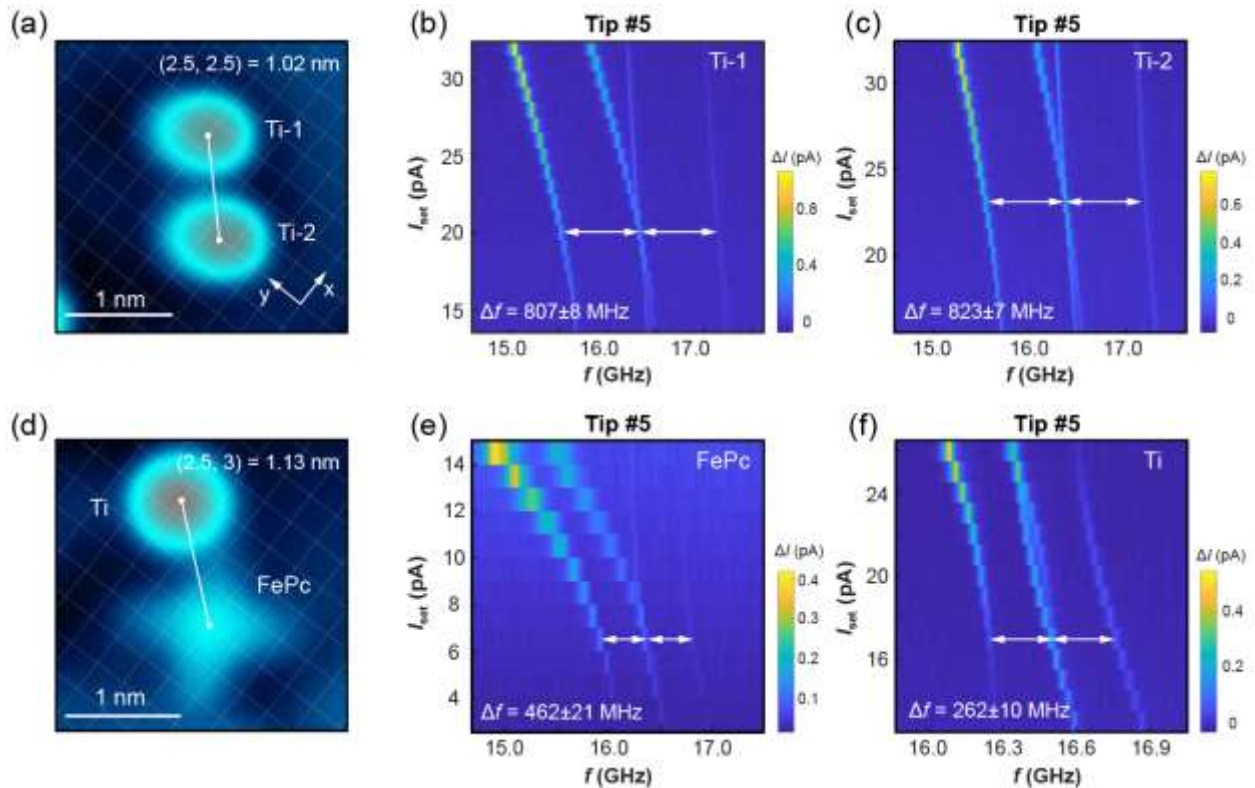
7 The doubling of the ESR peaks may also lead to the misinterpretation of the magnetic
 8 interaction energy of two coupled surface spins under certain circumstances, which we discuss in
 9 the following. To illustrate this behavior, we conducted ESR measurements of FePc-Ti dimers
 10 with closer inter-spin distance. In general, the ESR splitting (Δf) in a two-spin system, which
 11 has the same spin (FePc and Ti are both spin 1/2), is given by the total magnetic coupling energy
 12 between the two spins and becomes independent of the magnetic field (including B_{ex} and
 13 B_{tip}).^{18,32} Surprisingly, we found that the Δf of the FePc-Ti dimer appears to differ significantly
 14 depending on whether the tip is located on Ti or FePc. This result is reproducible by measuring
 15 dozens of FePc-Ti dimers with various tips (see supplementary material). We found that roughly
 16 50% of the ESR-active tips show identical ESR splitting within the error bars of our
 17 measurements on either spin. For the other ESR-active tips, the Δf reduces by almost half when
 18 the tip is positioned on the Ti atom of a FePc-Ti dimer compared to the FePc of the dimer, as

1 shown in Figure 3a. Here, tip#3 detected identical Δf on both FePc and Ti in the dimer (Figure
 2 3b and c) while Δf measured on Ti by tip#4 was almost half of that on FePc (Figure 3d and e).
 3 More examples are provided in Supplementary Information.



4
 5 **Figure 3. Magnetic coupling energy (Δf) of a FePc-Ti dimer measured with different tips.**
 6 (a) STM image of a (3, 1.5) FePc-Ti dimer. Scanning conditions: $V_{dc} = 150$ mV, $I_{set} = 8$ pA. (b-
 7 f) Current dependence of ESR spectra measured on (b, e) FePc and (c, f) Ti with (b, c) tip#3 and
 8 (d, e) tip#4, respectively. While Δf measured on Ti with tip#4 is almost half of the value
 9 measured on FePc, tip#3 measures nearly identical Δf no matter on which spin the tip is located.
 10 ESR conditions: $B_{ex} =$ (b, c) 565 mT, (d, e) 600 mT; $V_{dc} = 100$ mV; $V_{rf} =$ (b) 29 mV, (c) 35 mV,
 11 (d, f) 40 mV. The additional vertical lines anchored at fixed frequencies (14.7 and 17.7 GHz),
 12 which do not shift with current, originate from the low signal transmission in the cables.²³

1 Surprisingly, this tip-dependent behavior of Δf only appears in the hetero-dimers (*i.e.* FePc-Ti
 2 dimers) while Δf obtained on homo-dimers (*e.g.* Ti-Ti and FePc-FePc) showed no tip-
 3 dependence. In order to avoid ambiguity of using different tips in the hetero- and homo-dimers,
 4 we used the same tip #5 for the ESR measurement on a Ti-Ti dimer (Figure 4a) and a FePc-Ti
 5 (Figure 4d) dimer. We observed that Δf obtained on each spin in the Ti-Ti dimer are identical
 6 (Figure 4b and c) while Δf becomes half when the tip is atop the Ti compared to the FePc in the
 7 FePc-Ti dimer (Figure 4e and f), which is consistent with the observation above (Figure 3).
 8 Similar to Ti-Ti, Δf of the FePc-FePc dimers is always the same, regardless on which spin the
 9 tip is positioned on and is also the same when measured with different tips.²⁸ More comparisons
 10 of the hetero- and homo-dimers are presented in Figure S4.



11
 12 **Figure 4. Measuring the magnetic coupling strength of an iso-dimer (Ti-Ti) and a hetero-**
 13 **dimer (FePc-Ti) with the same tip (#5). (a, d) STM images of a Ti-Ti dimer having (2.5, 2.5)**

1 configuration and a FePc-Ti dimer having (2.5, 3) configuration. STM conditions: (a) $V_{\text{dc}} = 200$
 2 mV, $I_{\text{set}} = 8$ pA; (d) $V_{\text{dc}} = 200$ mV, $I_{\text{set}} = 10$ pA. (b, c) Current dependence of ESR spectra
 3 measured on each atom in the Ti-Ti dimer shown in (a). (e, f) Current dependence of ESR
 4 spectra obtained on the FePc-Ti dimer shown in (d) with the tip positioned on FePc and Ti,
 5 respectively. White arrows indicate the measured coupling energy (Δf) of the dimer. ESR
 6 conditions: $B_{\text{ex}} = 600$ mT; $V_{\text{dc}} = 100$ mV, $V_{\text{rf}} =$ (b, c) 25 mV, (e) 30 mV, (f) 20 mV.

7 To understand the tip-dependence of ESR splitting in the hetero-dimer, we simulated ESR
 8 spectra by solving a generalized Anderson impurity model. Our approach calculates the transport
 9 through a quantum impurity representing the coupled surface spins under time-dependent
 10 modulation.³³ The ESR spectrum is then simulated from the steady-state current calculated from
 11 the reduced density matrix of the system. Our model consists of two surface spins \mathbf{S}_{Ti} and \mathbf{S}_{FePc}
 12 as well as a time-averaged effective spin of the tip $\langle \mathbf{S}_{\text{tip}} \rangle$. Without loss of generality, we assume
 13 that the tip is located on top of Ti in our simulation, which allows us to write the impurity
 14 Hamiltonian as shown below.

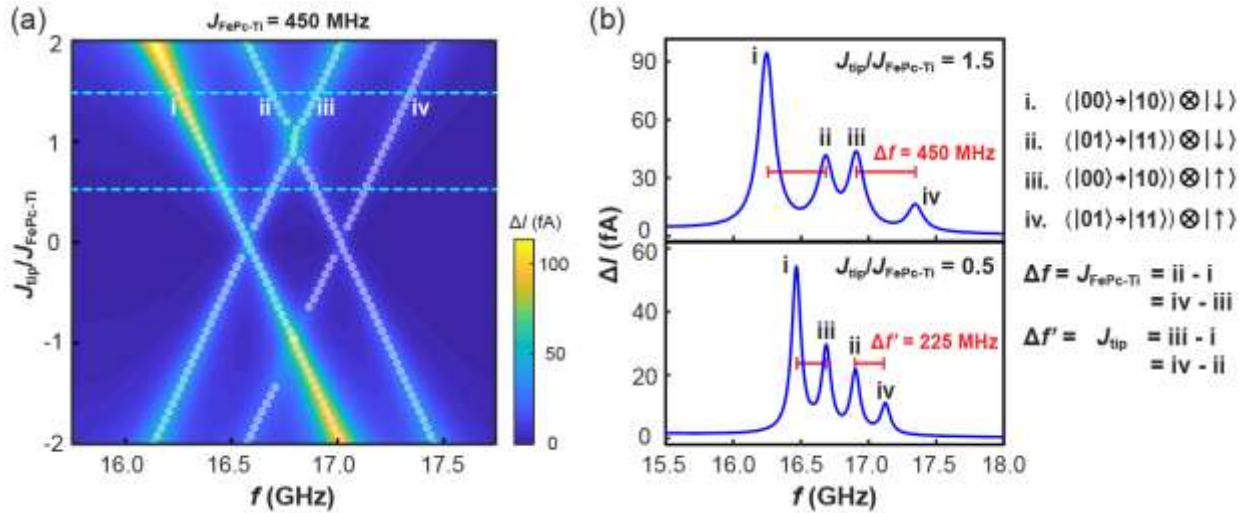
$$15 \quad H = g_{\text{Ti}} \mathbf{B}_{\text{ex}} \cdot \mathbf{S}_{\text{Ti}} + g_{\text{FePc}} \mathbf{B}_{\text{ex}} \cdot \mathbf{S}_{\text{FePc}} + J_{\text{FePc-Ti}} \mathbf{S}_{\text{FePc}} \cdot \mathbf{S}_{\text{Ti}} + J_{\text{tip}} \langle \mathbf{S}_{\text{tip}} \rangle \cdot \mathbf{S}_{\text{Ti}} \quad (2)$$

16 The first two terms describe the Zeeman energies of each individual surface spin, followed by
 17 the exchange-coupling term among the surface spins. The last term includes the exchange
 18 interaction between the surface spin (exemplified with Ti) and the tip. Without the tip, the
 19 Hamiltonian above describes two coupled spins of $S = 1/2$ which result in four allowed ESR
 20 transitions with a ESR splitting between the first (third) and second (fourth) peak that is equal to
 21 $J_{\text{FePc-Ti}}$.^{28,32}

22 Since the Zeeman energy is dominant in our case, the spins will mostly align with the z -axis
 23 while $\langle \mathbf{S}_{\text{tip}} \rangle$ is required to have components in the direction perpendicular to the quantization

1 axis to drive ESR.³³ In the following discussion, it is sufficient to consider only two states of the
2 tip, which will lead to a doubling of the ESR transitions with four for each tip state. Due to
3 degeneracies, less than eight peaks will be generally visible in the ESR spectrum. In addition,
4 separating transitions stemming from a change in the tip state can be difficult if $\mathbf{B}_{\text{tip}}g\mu_B =$
5 $J_{\text{tip}}\langle\mathbf{S}_{\text{tip}}\rangle \approx J_{\text{FePc-Ti}}\mathbf{S}_{\text{FePc}}$. To show this, we calculated a series of spectra as a function of the
6 ratio between J_{tip} and $J_{\text{FePc-Ti}}$ (Figure 5). When $|J_{\text{tip}}/J_{\text{FePc-Ti}}|$ is less than 1, some transitions of
7 the spectra for the tip being up or down overlap, leading to a misinterpretation of transitions
8 belonging to different sub-spaces of the tip states. When $|J_{\text{tip}}/J_{\text{FePc-Ti}}| > 1$, this misinterpretation
9 can be avoided as adjacent peaks belong to the same tip state (Figure 5b) and only under this
10 condition can the interaction strength of the surface spins be extracted reliably from the ESR
11 spectrum.

12 The above simulations illustrate how a change in the exchange interaction strength between tip
13 and surface spin can lead to a misinterpretation of the ESR splitting, resulting in an extracted
14 exchange energy that is different from the intrinsic coupling energy of a spin dimer. Considering
15 the distance between the tip and surface spin and the distance between two surface spins are
16 comparable in the experiment, J_{tip} can be comparable or larger than $J_{\text{FePc-Ti}}$. Given the
17 difference (~ 0.17 nm, Figure S5) in the apparent height of FePc and Ti adsorbed on surface, the
18 exchange interaction energy between each surface spin and the tip can be drastically different²⁹,
19 causing the site-dependent ESR splitting in measurement. Notably, our model is applicable to
20 both hetero- and homo-dimer case. The measured ESR splitting of a homo-dimer may vary if
21 different tips are used, which has not been found in our experiments.



1
2 **Figure 5. Simulated ESR spectra concerning the relative amplitude of J_{tip} vs. $J_{\text{FePC-Ti}}$.** (a)
3 ESR peak intensities for different J_{tip} strength as a function of the frequency. In all calculations
4 the intrinsic coupling energy of the surface spins is set to $J_{\text{FePC-Ti}} = 450$ MHz. The 2D map
5 shows regions where resonances emerge between consecutive peaks when $|J_{\text{tip}}/J_{\text{FePC-Ti}}|$ is
6 between 0 and 1. This leads to the misinterpretation of the coupling energy as described in the
7 main text. AFM ($J_{\text{tip}} > 0$) or FM coupling ($J_{\text{tip}} < 0$) of the tip lead to the same conclusion. (b)
8 Representative ESR spectra calculated with large (1.5, upper left panel) and mediate (0.5, lower
9 left panel) $J_{\text{tip}}/J_{\text{FePC-Ti}}$. The right panel lists the four ESR transitions corresponding to each
10 resonance peak. Notably, fewer ESR peaks than those shown in (a) might be observed in an
11 experiment due to weak intensities. When $|J_{\text{tip}}/J_{\text{FePC-Ti}}|$ is between 0 and 1, adjacent peaks
12 belong to different sub-spaces of the tip state and therefore $\Delta f'$ does not correspond to $J_{\text{FePC-Ti}}$.
13 For $|J_{\text{tip}}/J_{\text{FePC-Ti}}| \geq 1$ adjacent peaks will always belong to the same sub-space of the tip state.

14 CONCLUSION

15 In this ESR-STM work, we have shown the importance of considering the role of the magnetic
16 tip in hetero-spin systems. We found that the ESR signals in hetero-spin systems require a

1 careful examination when the interaction energy between the tip and one surface spin is of the
2 same order as the interaction energy between the surface spins. Our model enables us to clearly
3 assign the transitions of all ESR peaks. In particular, we investigated FePc-Ti hetero-dimers, a
4 system of two coupled spins of $S = 1/2$, in which each spin interacts differently with the magnetic
5 tip and results in site-dependent ESR splitting. Our work highlights that controlling the tip states
6 via site-dependent ESR could be a viable pathway to selectively drive spin transitions in
7 heterogeneous multi-spin systems on surfaces.

8 METHODS

9 Our experiments were performed in a commercial low-temperature STM (Unisoku,
10 USM1300). The Ag(100) substrate was pretreated by alternating Ar^+ sputtering and annealing
11 cycles to obtain atomically flat terraces. MgO was prepared by evaporating magnesium onto
12 clean Ag(100) surface kept at 400°C in an oxygen atmosphere of 1.1×10^{-6} torr. FePc molecules
13 were deposited onto MgO at room-temperature while Ti and Fe atoms were deposited onto cold
14 samples. The thickness of MgO layers grown on Ag(100) was determined by performing point-
15 contact dI/dz spectroscopy on individual Fe atoms and the experiments were performed at two
16 monolayers of MgO.³⁴ All STM and ESR measurements were conducted at 2 K and the external
17 magnetic field was applied out-of-plane.

18 The ac voltage of radio-frequency (V_{rf}) was generated by a signal generator (Keysight,
19 E8257D) and introduced to the tip side of the tunneling junction through a bias tee. The dc bias
20 (V_{dc}) was added with respect to the sample and kept continuously on during the ESR
21 measurement. V_{rf} was modulated at 95 Hz for the sake of reading out the ESR signal by lock-in
22 technique. The sample was connected to an electrometer to read out the tunneling current and the
23 ESR signal.

1 The theoretical calculations were performed based on the transport approach in Ref. 35. To
2 simulate the ESR current, a quantum master equation of the reduced density matrix was solved
3 under the assumption of weak coupling between the quantum impurity (spin Hamiltonian of the
4 atoms or molecules plus the effective tip spin, Eq. (2)) and two electron baths, representing the
5 tip and substrate. In our simulations, the tip was spin-polarized by 45%. The coupling between
6 the baths and impurity contains a periodic change of the potential barrier under a radio frequency
7 voltage. The current through the impurity is computed from the reduced density matrix elements.

8 It is important to emphasize that in Eq. (2) all quantities are vectors, including x, y, and z
9 components. The x and y components are essential to provide the necessary mixing of the spin
10 states involved. The calculations in Figure 5 used the following parameters, which were chosen
11 similar to the experiment: $\mathbf{B}_{\text{ex}} = 0.6(\cos\theta, 0, \sin\theta)$, $\theta = 80^\circ$, $J_{\text{FePc-Ti}} = \Delta f = 450$ MHz, $g_{\text{Ti}} =$
12 $g_{\text{FePc}} = 2$. The angle θ is expressed with respect to the in-plane direction. We used $\langle \mathbf{S}_{\text{tip}} \rangle = \pm$
13 $1/2$ but generally only the product of $J_{\text{tip}} \langle \mathbf{S}_{\text{tip}} \rangle$ is relevant. Notably, some in-plane component
14 may result in additional ESR splitting which is not considered in our model.

15 ASSOCIATED CONTENT

16 **Supporting Information.** The Supporting Information is available free of charge at
17 <https://pubs.acs.org>.

18 Comparison of ESR spectra measured by a stable and a bistable tip, characterizing different tip
19 states in ESR-STM by measuring isolated spins, tip-dependent ESR splitting in FePc-Ti dimers,
20 Comparison of ESR splitting measured in homo-dimers and hetero-dimers (PDF)

21 AUTHOR INFORMATION

1 **Corresponding Authors**

2 *Andreas J. Heinrich - *Center for Quantum Nanoscience, Institute for Basic Science (IBS), Seoul*
3 *03760, Republic of Korea; Department of Physics, Ewha Womans University, Seoul 03760,*
4 *Republic of Korea; orcid.org/0000-0001-350 6204-471X; Email: heinrich.andreas@qns.science*

5 *Taeyoung Choi - *Department of Physics, Ewha Womans University, Seoul 03760, Republic of*
6 *Korea; Email: tchoi@ewha.ac.kr*

7 **Author Contributions**

8 X.Z. and T.C. designed the project. X.Z. and Y.W. performed the experiments. J.R.-G. and C.W.
9 developed the model and carried out calculations. H.A. contributed to discussions. X.Z. and J.R.-
10 G. wrote the manuscript with help of all authors. T.C. and A.J.H. advised the project process.

11 **Data availability**

12 All data that support the findings of this study are available in this manuscript and its
13 Supplementary Information, or from the corresponding authors on reasonable request.

14 **Notes**

15 The authors declare no competing financial interest.

16 **ACKNOWLEDGMENT**

17 All authors acknowledge support from the Institute for Basic Science under grant IBS-R027-
18 D1. H.A. acknowledges financial support from ANR TOSCA Grant No. ANR-22-CE30-0037-
19 01. X.Z acknowledges financial support from the National Natural Science Foundation of China
20 (grant agreement No. 22202074) and “the Fundamental Research Funds for the Central
21 Universities”. We also thank Nicolás Lorente for the fruitful discussions.

1 REFERENCES

2 [1] Schirhagl, R., Chang, K., Loretz, M., Degen, C. L. Nitrogen-vacancy centers in diamond:
3 nanoscale sensors for physics and biology. *Annu. Rev. Phys. Chem.* **2014**, *65*, 83–105.

4 [2] Awschalom, D. D.; Hanson, R.; Wrachtrup, J.; Zhou, B. B. Quantum technologies with
5 optically interfaced solid-state spins. *Nat. Photonics* **2018**, *12*, 516–527.

6 [3] Debnath, S.; Linke, N. M.; Figgatt, C.; Landsman, K. A.; Wright, K.; Monroe, C.
7 Demonstration of a small programmable quantum computer with atomic qubits. *Nature* **2016**,
8 *536*, 63–66.

9 [4] Monroe, C.; Campbell, W. C.; Duan, L.-M.; Gong, Z.-X.; Gorshkov, A. V.; Hess, P. W.;
10 Islam, R.; Kim, K.; Linke, N. M.; Pagano, G.; Richerme, P.; Senko, C.; Yao, N. Y.
11 Programmable quantum simulations of spin systems with trapped ions. *Rev. Mod. Phys.* **2021**,
12 *93*, 025001.

13 [5] Burkard, G.; Gullans, M. J.; Mi, X.; Petta, J. R. Superconductor–semiconductor hybrid-
14 circuit quantum electrodynamics. *Nat. Rev. Phys.* **2020**, *2*, 129–140.

15 [6] Tanttu, T.; Hensen, B.; Chan, K. W.; Yang, C. H.; Huang, W. W.; Fogarty, M.; Hudson, F.;
16 Itoh, K.; Culcer, D.; Laucht, A.; Morello, A.; Dzurak, A. Controlling spin-orbit interactions in
17 silicon quantum dots using magnetic field direction. *Phys. Rev. X* **2019**, *9*, 021028.

18 [7] Gehring, P.; Thijssen, J. M.; van der Zant, H. S. J. Single-molecule quantum-transport
19 phenomena in break junctions. *Nat. Rev. Phys.* **2019**, *1*, 381–396.

20 [8] Vincent, R.; Klyatskaya, S.; Ruben, M.; Wernsdorfer, W.; Balestro, F. Electronic read-out
21 of a single nuclear spin using a molecular spin transistor. *Nature* **2012**, *488*, 357–360.

- 1 [9] Baumann, S.; Paul, W.; Choi, T.; Lutz, C. P.; Ardavan, A.; Heinrich, A. J. Electron
2 paramagnetic resonance of individual atoms on a surface. *Science* **2015**, *350*, 417–420.
- 3 [10] Yang, K.; Paul, W.; Phark, S.-H.; Willke, P.; Bae, Y.; Choi, T.; Esat, T.; Ardavan, A.;
4 Heinrich, A. J.; Lutz, C. P. Coherent spin manipulation of individual atoms on a surface. *Science*
5 **2019**, *366*, 509–512.
- 6 [11] Willke, P.; Bilgeri, T.; Zhang, X.; Wang, Y.; Wolf, C.; Aubin, H.; Heinrich, A.; Choi, T.
7 Coherent spin control of single molecules on a surface. *ACS Nano* **2021**, *15*, 17959–17965.
- 8 [12] Seifert, T. S.; Kovarik, S.; Nistor, C.; Persichetti, L.; Stepanow, S.; Gambardella, P.
9 Single-atom electron paramagnetic resonance in a scanning tunneling microscope driven by a
10 radio-frequency antenna at 4 K. *Phys. Rev. Res.* **2020**, *2*, 013032.
- 11 [13] Steinbrecher, M.; van Weerdenburg, W. M. J.; Walraven, E. F.; van Mellekom, N. P. E.;
12 Gerritsen, J. W.; Natterer, F. D.; Badrtdinov, D. I.; Rudenko, A. N.; Mazurenko, V. V.;
13 Katsnelson, M. I.; van der Avoird, A.; Groenenboom, G. C.; Khajetoorians, A. A. Quantifying
14 the interplay between fine structure and geometry of an individual molecule on a surface. *Phys.*
15 *Rev. B* **2021**, *103*, 155405.
- 16 [14] Veldman, L. M.; Farinacci, L.; Rejali, R.; Broekhoven, R.; Gobeil, J.; Coffey, D.; Ternes,
17 M.; Otte, A. F. Free coherent evolution of a coupled atomic spin system initialized by electron
18 scattering, *Science* **2021**, *372*, 964–968.
- 19 [15] Drost, R.; Uhl, M.; Kot, P.; Siebrecht, J.; Schmid, A.; Merkt, J.; Siegel, M.; Kieler, O.;
20 Kleiner, R.; Ast, C. R. Combining electron spin resonance spectroscopy with scanning tunneling
21 microscopy at high magnetic fields. *Rev. Sci. Instrum.* **2022**, *93*, 043705.

- 1 [16] Kovarik, S.; Robles, R.; Schlitz, R.; Seifert, T. S.; Lorente, N.; Gambardella, P.;
2 Stepanow, S. Electron paramagnetic resonance of alkali metal atoms and dimers on ultrathin
3 MgO. *Nano Lett.* **2022**, *22*, 4176–4181.
- 4 [17] Kawaguchi, R.; Hashimoto, K.; Kakudate, T.; Katoh, K.; Yamashita, M.; Komeda, T.
5 Spatially resolving electron spin resonance of π -radical in single-molecule magnet. *Nano Lett.*
6 **2023**, *23*, 213–219.
- 7 [18] Choi, T.; Paul, W.; Rolf-Pissarczyk, S.; Macdonald, A. J.; Natterer, F. D.; Yang, K.;
8 Willke, P.; Lutz, C. P.; Heinrich, A. J. Atomic-scale sensing of the magnetic dipolar field from
9 single atoms. *Nat. Nanotechnol.* **2017**, *12*, 420–424.
- 10 [19] Yang, K.; Phark, S.-H.; Bae, Y.; Esat, T.; Willke, P.; Ardavan, A.; Heinrich, A. J.; Lutz,
11 C. P. Probing resonating valence bond states in artificial quantum magnets. *Nat. Commun.* **2021**,
12 *12*, 993.
- 13 [20] Willke, P.; Bae, Y.; Yang, K.; Lado, J. L.; Ferrón, A.; Choi, T.; Ardavan, A.; Fernández-
14 Rossier, J.; Heinrich, A. J.; Lutz, C. P. Hyperfine interaction of individual atoms on a surface.
15 *Science* **2018**, *362*, 336–339.
- 16 [21] Yang, K.; Willke, P.; Bae, Y.; Ferrón, A.; Lado, J. L.; Ardavan, A.; Fernández-Rossier, J.;
17 Heinrich, A. J.; Lutz, C. P. Electrically controlled nuclear polarization of individual atoms. *Nat.*
18 *Nanotechnol.* **2018**, *13*, 1120–1125.
- 19 [22] Seifert, T. S.; Kovarik, S.; Juraschek, D. M.; Spaldin, N. A.; Gambardella, P.; Stepanow,
20 S. Longitudinal and transverse electron paramagnetic resonance in a scanning tunneling
21 microscope. *Sci. Adv.* **2020**, *6*, eabc5511.

- 1 [23] Paul, W.; Baumann, S.; Lutz, C. P.; Heinrich, A. J. Generation of constant-amplitude
2 radio-frequency sweeps at a tunnel junction for spin resonance STM. *Rev. Sci. Instrum.* **2016**, *87*,
3 074703.
- 4 [24] Loth, S.; von Bergmann, K.; Ternes, M.; Otte, A. F.; Lutz, C. P.; Heinrich, A. J.
5 Controlling the state of quantum spins with electric currents. *Nat. Phys.* **2010**, *6*, 340–344.
- 6 [25] Kim, J.; Jang, W.-J.; Bui, T. H.; Choi, D.-J.; Wolf, C.; Delgado, F.; Chen, Y.; Krylov, D.;
7 Lee, S.; Yoon, S.; Lutz, C. P.; Heinrich, A. J.; Bae, Y. Spin resonance amplitude and frequency
8 of a single atom on a surface in a vector magnetic field. *Phys. Rev. B* **2021**, *104*, 174408.
- 9 [26] Yang, K.; Paul, W.; Natterer, F. D.; Lado, J. L.; Bae, Y.; Willke, P.; Choi, T.; Ferrón, A.;
10 Fernández-Rossier, J.; Heinrich, A. J.; Lutz, C. P. Tuning the exchange bias on a single atom
11 from 1 mT to 10 T. *Phys. Rev. Lett.* **2019**, *122*, 227203.
- 12 [27] Seifert, T. S.; Kovarik, S.; Gambardella, P.; Stepanow, S. Accurate measurement of
13 atomic magnetic moments by minimizing the tip magnetic field in STM-based electron
14 paramagnetic resonance. *Phys. Rev. Res.* **2021**, *3*, 043185.
- 15 [28] Zhang, X.; Wolf, C.; Wang, Y.; Aubin, H.; Bilgeri, T.; Willke, P.; Heinrich, A. J.; Choi,
16 T. Electron spin resonance of single iron phthalocyanine molecules and role of their non-
17 localized spins in magnetic interactions. *Nat. Chem.* **2022**, *14*, 59–65.
- 18 [29] Willke, P.; Singha, A.; Zhang, X.; Esat, T.; Lutz, C. P.; Heinrich, A. J.; Choi, T. Tuning
19 single-atom electron spin resonance in a vector magnetic field. *Nano Lett.* **2019**, *19*, 8201–8206.
- 20 [30] Yan, S.; Choi, D.-J.; Burgess, J. A. J.; Rolf-Pissarczyk, S.; Loth, S. Control of quantum
21 magnets by atomic exchange bias. *Nat. Nanotechnol.* **2015**, *10*, 40–45.

1 [31] Singha, A.; Willke, P.; Bilgeri, T.; Zhang, X.; Brune, H.; Donati, F.; Heinrich, A. J.; Choi,
2 T. Engineering atomic-scale magnetic fields by dysprosium single atom magnets. *Nat. Commun.*
3 **2021**, *12*, 4179.

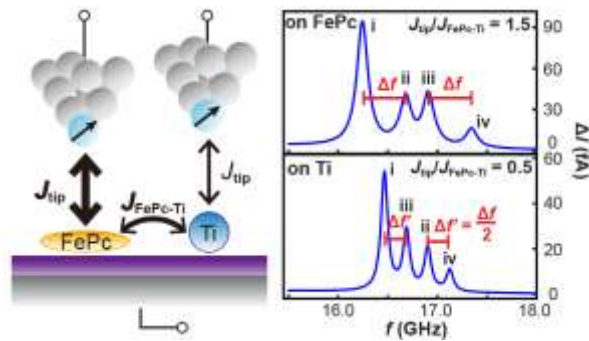
4 [32] Yang, K.; Bae, Y.; Paul, W.; Natterer, F. D.; Willke, P.; Lado, J. L.; Ferrón, A.; Choi, T.;
5 Fernández-Rossier, J.; Heinrich, A. J.; Lutz, C. P. Engineering the eigenstates of coupled spin-
6 $1/2$ atoms on a surface. *Phys. Rev. Lett.* **2017**, *119*, 227206.

7 [33] Willke, P.; Yang, K.; Bae, Y.; Heinrich, A. J.; Lutz, C. P. Magnetic resonance imaging of
8 single atoms on a surface. *Nat. Phys.* **2019**, *15*, 1005–1010.

9 [34] Paul, W.; Yang, K.; Baumann, S.; Romming, N.; Choi, T.; Lutz, C. P.; Heinrich, A. J.
10 Control of the millisecond spin lifetime of an electrically probed atom. *Nat. Phys.* **2017**, *13*, 403–
11 407.

12 [35] Reina-Gálvez, J.; Lorente, N.; Delgado, F.; Arrachea, L. All-electric electron spin
13 resonance studied by means of Floquet quantum master equations. *Phys. Rev. B* **2021**, *104*,
14 245435.

15 Table of Contents



16

17

Tip-influenced electron spin resonance splitting on hetero-dimers